Right-handed neutrino pair production via second-generation leptoquarks

Arvind Bhaskar,[1, *] Yash Chaurasia,[1, †] Kuldeep Deka,[2, ‡] Tanumoy
Mandal,[3, §] Subhadip Mitra,[1, ¶] and Ananya Mukherjee[4, **]

[1]*Center for Computational Natural Sciences and Bioinformatics,
International Institute of Information Technology, Hyderabad 500 032, India*
[2]*Department of Physics and Astrophysics, University of Delhi, Delhi 110 007, India*
[3]*Indian Institute of Science Education and Research Thiruvananthapuram, Vithura, Kerala, 695 551, India*
[4]*Theory Division, Saha Institute of Nuclear Physics, 1/AF Bidhannagar, Kolkata 700 064, India*

No direct experimental constraints exist on Leptoquark (LQ) couplings with quarks and right-handed neutrinos (RHNs). If a LQ dominantly couples to RHNs, it can leave unique signatures at the LHC. The RHNs can be produced copiously from LQ decays as long as they are lighter than the LQs. LQ-induced RHN production has never been searched for in experiments. This channel can act as a simultaneous probe for RHNs and LQs that dominantly couple to RHNs. In this paper, we consider all possible charge-2/3 and 1/3 scalar and vector LQs that dominantly couple to second-generation quarks and RHN. We study the pair and single productions of TeV-scale LQs and their subsequent decay to sub-TeV RHNs, realised in the inverse seesaw framework. We also consider RHN pair production through a t-channel LQ exchange. The single LQ production and t-channel contributions can be significant for large LQ-RHN-quark couplings. We systematically combine events from these processes leading to a pair of RHNs plus jets to study the prospects of LQ-assisted RHN pair production. We analyse the monolepton and opposite-sign dilepton final states and estimate the discovery reach at the high-luminosity LHC.

I. INTRODUCTION

The neutrino oscillation data provide vital evidence for the presence of physics beyond the Standard Model (SM) by pointing towards the neutrino masses. However, probing the neutrino sector at particle colliders is not simple—due to their elusive nature, the light neutrinos pass through the detectors undetected. Generally, one considers heavy right-handed neutrinos (RHNs, ν_R's) to generate light-neutrino masses through the seesaw mechanism. Observing RHNs at the Large Hadron Collider (LHC) would be an important milestone since it could shed light on the neutrino mass generation mechanism and various serious issues like the dark matter problem, matter-antimatter asymmetry, etc. In principle, the LHC could probe RHNs if they are within the TeV range. However, a straightforward application of the vanilla seesaw mechanism (Type-I) [1, 2] puts the RHNs several orders of magnitude above the TeV scale.

There are other mechanisms to generate the masses—like the inverse seesaw mechanism (ISM) [3, 4]—where the RHNs can be within the reach of the LHC. But, even the TeV-scale RHNs are not easy to produce at the LHC (see Ref. [5] for the prospect study of RHNs at e^+e^- colliders). Since they are singlet under the SM gauge group, they interact feebly with the SM fields through their small overlaps with the left-handed neutrinos generated after the electroweak symmetry breaking. RHNs can be produced through the decay of another particle like W' [6, 7], Z' [8–11], etc. Since the LHC is a hadron collider, RHNs can also be produced through an intermediary that connects with the strong sector. In this paper, we consider one that fits naturally in this picture, namely, the leptoquark (LQ).

LQs are hypothetical coloured scalar or vector bosons with both baryon and lepton numbers. Hence, they can act as connectors between the baryon and lepton sectors. They appear in various beyond-the-SM theories like the Pati-Salam models [12], Grand Unified Theories [13], various compositeness theories [14], or R-parity-violating Supersymmetry [15], etc. Nowadays, they are popular in the literature for explaining various experimental anomalies, like the ones seen in $R_{D^{(*)}}$, $(g-2)_\mu$, W-mass, etc. [16–26]. The phenomenology of LQs and their discovery prospects at different colliders can be found in Refs. [27–38].

The LHC has an ongoing LQ-search program. Both ATLAS and CMS Collaborations are looking for single and pair productions of LQs in various combinations of leptons (ℓ or ν_L) and jets (light or t jet) in the final states. The current mass-exclusion limits on scalar and vector LQs go up to 1.73 [39] and 1.98 [40] TeV, respectively. There are also indirect bounds on LQ couplings (LQ-quark-lepton) from the high-p_T dilepton or monolepton with missing energy data [19, 25]. A LQ can simultaneously couple with a SM quark and a RHN. However, none of the direct or indirect bounds concerns this coupling. A LQ can decay to a RHN+jet final state if the RHN is lighter than the LQ. If the LQ decays exclusively (or predominantly) through this mode, it becomes unrestricted by all the direct or indirect bounds. In other words, a large part of the LQ parameter space remains unexplored and unrestricted by the LHC.

In this paper, we utilise this freedom to study the production of RHNs via LQs at the hadron collider (similar or related phenomenological studies are found in Refs. [41–45]). If we assume the LQ couples with no other leptons except the RHNs, there are two possible production processes for the RHNs—they can come from LQ decays, or they can be directly pair produced by t-channel LQ exchanges in the quark fusion mode. As we discuss later, normally, the LQ-decay mode is more promising than the t-channel LQ

* arvind.bhaskar@research.iiit.ac.in
† yash.chaurasia@research.iiit.ac.in
‡ kuldeepdeka.physics@gmail.com
§ tanumoy@iisertvm.ac.in
¶ subhadip.mitra@iiit.ac.in
** ananyatezpur@gmail.com

exchange if the RHNs are lighter than the LQ. One reason is that LQs can be produced copiously through strong interaction. Secondly, the cross-section of the t-channel LQ-exchange process is susceptible to the LQ-quark-lepton coupling (goes as the fourth power); unless the coupling is of order one or larger, its cross-section is relatively smaller. Hence, in this paper, we mainly focus on RHN production through LQ decay.

For our purpose, we consider a setup where the light neutrinos get their masses through the ISM. In the ISM, there are three RHNs (one for each generation) and three extra neutral fermions (S_{L_i} with $i \in \{1,2,3\}$ being the generation index, all singlets under the SM gauge group). Due to these extra fermions, the RHNs can have (sub-)TeV-range masses. We are interested in the parameter regions where the RHNs are lighter than LQs so they can decay exclusively through the RHN+jet decay mode. For the LHC to detect their signatures, the RHNs should not be long-lived and decay to SM particles within the detectors. Generally, the strongest collider bounds on the RHNs come from the searches for the same-sign dilepton pairs, the signature of the Majorana nature of the RHNs. However, these bounds do not affect our analysis as the RHNs are pseudo-Dirac types in ISM. They decay mainly through the $\nu_R \to W^\pm \ell^\mp$ and $\nu_R \to Z/h\,\nu_\ell$ processes in roughly $2:1:1$ ratio.

Generally, LQs can have inter or intra-generational couplings (i.e., the quark and the lepton that couple to a LQ need not be of the same generation). LQs that dominantly couple to third-generation fermions should be separately searched for from those that mostly couple to the lighter-generation fermions [33, 35, 46]. This is because the detection strategies for the third-generation fermions differ significantly from the first two generations. There are also significant differences in the single and indirect LQ-production (i.e., t-channel LQ exchange) cross-sections depending on whether they couple to the first or second-generation quarks. This happens because the first-generation quarks have the largest parton distribution functions (PDFs). For the LHC analysis, we mainly consider second-generation interactions, i.e., LQs essentially decay to a second-generation quark and a second-generation RHN (i.e., second-generation LQs), and the RHN decays to produce a second-generation lepton in the final state. There are two reasons for this choice. First, the muon-detection efficiency is better than the electron detection at the LHC. Second, and more importantly, the second-generation case gives us a conservative estimate of the prospects of this channel. Due to the larger PDFs of the up and down quarks, the LHC discovery reach for mostly first-generation interactions would be better. We shall report the prospects for the first and third-generation cases separately.

The paper is organised as follows. We review the ISM in the next section. In Sec. III, we list the possible LQ models with RHN-decay mode and introduce some simple phenomenological models. In Sec. IV, we discuss the signals and the backgrounds and present our results in Sec. V. Finally, we conclude in Sec. VI.

II. THE INVERSE SEESAW MECHANISM

We can write the neutrino-sector interactions as

$$-\mathcal{L} \supset \lambda_\nu^i \, \overline{L_i} \widetilde{H} \, \nu_{R_i} + M_R \, \overline{\nu_{R_i}} S_{L_i} + \frac{1}{2} \mu \, \overline{S_{L_i}^c} S_{L_i} + \text{H.c.}, \qquad (1)$$

where i is the generation index, L_i is the ith lepton doublet, $\widetilde{H} = i\sigma_2 H^*$, and the superscript c denotes charge conjugation. Sterile neutrinos are denoted as S_L. They are SM singlets and carry the lepton number $L = 1$. Similarly, RHNs also have $L = 1$. The S_L fields interact with ν_R but not directly with the SM leptons. However, tiny interactions can arise after mass mixing. In the $\{\nu_L^c \ \nu_R \ S_L^c\}$ basis, the neutrino mass matrix can be written as

$$\mathbf{M}_\nu = \begin{pmatrix} \mathbf{0} & \mathbf{m}_D & \mathbf{0} \\ \mathbf{m}_D^T & \mathbf{0} & \mathbf{M}_R \\ \mathbf{0} & \mathbf{M}_R^T & \mu \end{pmatrix}, \qquad (2)$$

where all of $\mathbf{m}_D, \mathbf{M}_R$ and μ are 3×3 mass matrices. The light-neutrino masses are obtained after block diagonalising the mass matrix as the following,

$$\mathbf{m}_\nu \approx \mathbf{m}_D (\mathbf{M}_R^T)^{-1} \mu \mathbf{M}_R^{-1} \mathbf{m}_D^T. \qquad (3)$$

For the heavy components, the 6×6 mass matrix in the $(\mathbf{N}_R \ \mathbf{S})$ basis can be written as

$$\mathbf{M}_\nu^{6 \times 6} = \begin{pmatrix} \mathbf{0} & \mathbf{M}_R \\ \mathbf{M}_R^T & \mu \end{pmatrix}, \qquad (4)$$

where $\mu \sim$ keV is the lepton-number violating scale that essentially acts as the source of tiny non-degeneracy among the final pseudo-Dirac pairs.

For us, the essential point is our collider study is largely insensitive to the parameters in the neutrino sector (like $\mathbf{m}_D, \mathbf{M}_R, \mu$ etc.) except the mass and decays of the second-generation RHN. Hence, we do not need any specially tuned parameter as sub-TeV RHNs decaying to $W^\pm \ell^\mp$ and $Z/h\,\nu_\ell$ final states are easily found in the allowed parameter space (see, e.g., [7, 11]).

III. SCALAR AND VECTOR LEPTOQUARK MODELS

We list the LQs—scalars (sLQ) and vectors (vLQs)—with interactions with the RHNs [47]. We ignore the diquark operators to bypass the proton-decay constraints.

A. Scalar LQs

■ $\widetilde{R}_2 = (\overline{\mathbf{3}}, \mathbf{2}, 1/6)$: The interaction of $\widetilde{R}_2$ can be written as follows,

$$\mathcal{L} \supset \tilde{y}_{2ij}^{\overline{LR}} \, \bar{Q}_L^{i,a} \tilde{R}_2^a \nu_R^j + \text{H.c.}, \qquad (5)$$

where $\bar{Q}_L$ denotes the left-handed quark doublet, $a, b = 1, 2$ are the $SU(2)$ indices, and $\varepsilon = i\sigma^2$. The terms relevant to our analysis are

$$\mathcal{L} \supset \tilde{y}_{2\,ii}^{\overline{LR}} \, \bar{u}_L^i \nu_R^i \tilde{R}_2^{2/3} + \tilde{y}_{2\,ii}^{\overline{LR}} \, \bar{d}_L^i \nu_R^i \tilde{R}_2^{-1/3} + \text{H.c.} \qquad (6)$$

■ $S_1 = (\bar{\mathbf{3}}, \mathbf{1}, 1/3)$: The only relevant term in the interaction Lagrangian of S_1 is

$$\mathscr{L} \supset - \bar{y}^{RR}_{1ii} \, \bar{d}^{C\,i}_R S_1 v^i_R + \text{H.c.} \tag{7}$$

■ $\bar{S}_1 = (\bar{\mathbf{3}}, \mathbf{1}, -2/3)$: The relevant term is

$$\mathscr{L} \supset + \bar{y}^{\overline{RR}}_{1ii} \, \bar{u}^{C\,i}_R \bar{S}_1 v^i_R + \text{H.c.} \tag{8}$$

B. Vector LQs

■ $\tilde{V}_2 = (\bar{\mathbf{3}}, \mathbf{2}, -1/6)$: The RHN interaction of $\tilde{V}_2$ can be written as

$$\mathscr{L} \supset \tilde{x}^{\overline{LR}}_{2ij} \bar{Q}^{C\,i,a}_L \gamma^\mu \varepsilon^{ab} \tilde{V}^b_{2,\mu} v^j_R + \text{H.c.}, \tag{9}$$

which gives us the terms relevant to our analysis:

$$\mathscr{L} \supset \tilde{x}^{\overline{LR}}_{2\,ii} \, \bar{u}^{C\,i}_L \gamma^\mu v^i_R \tilde{V}^{-2/3}_{2,\mu} - \tilde{x}^{\overline{LR}}_{2\,ii} \, \bar{d}^{C\,i}_L \gamma^\mu v^i_R \tilde{V}^{-1/3}_{2,\mu} + \text{H.c.} \tag{10}$$

■ $\bar{U}_1 = (\bar{\mathbf{3}}, \mathbf{1}, -1/3)$: The only relevant term for $\bar{U}_1$ is as follows,

$$\mathscr{L} \supset \bar{x}^{\overline{RR}}_{1ii} \, \bar{d}^i_R \gamma^\mu \bar{U}_{1,\mu} v^i_R + \text{H.c.} \tag{11}$$

■ $U_1 = (\bar{\mathbf{3}}, \mathbf{1}, 2/3)$: The relevant term for U_1 is as follows,

$$\mathscr{L} \supset \bar{x}^{\overline{RR}}_{1ii} \, \bar{u}^i_R \gamma^\mu \bar{U}_{1,\mu} v^i_R + \text{H.c.} \tag{12}$$

C. Simple models

We can generically express the LQ interactions in terms of some phenomenological Lagrangians in the spirit of Refs. [33, 35, 46] as

$$\mathscr{L} \supset \lambda_1 \bar{d}_L v_R \phi_1 + \lambda_2 \bar{u}_L v_R \phi_2 + \text{H.c.}, \tag{13}$$

$$\mathscr{L} \supset \Lambda_1 \bar{d}_R (\gamma \cdot \chi_1) v_R + \Lambda_2 \bar{u}_R (\gamma \cdot \chi_2) v_R + \text{H.c.}, \tag{14}$$

where d and u represent generic down and up-type quarks, respectively and ϕ_n, χ_n denote an (absolute) charge-$n/3$ LQ. If we assume no mixing among the right-handed quarks, the interactions of the weak-singlet LQs (S_1, $\bar{S}_1$, U_1, or $\bar{U}_1$) can be modelled by considering only one nonzero λ_n or Λ_n (flavour diagonal)—we assume these couplings are real for simplicity. However, to model the doublet ($\tilde{R}_2$ or $\tilde{V}_2$) interactions, we have to set $\lambda_1 = \lambda_2$ or $\Lambda_1 = -\Lambda_2$ and, depending on whether the LQ interaction is aligned with the up-type or down-type quarks, replace d^i_L (where i indicates the generation) by $[V_{\text{CKM}}]_{ij} d^j_L$ or u^i_L by $[V^\dagger_{\text{CKM}}]_{ij} u^j_L$ where V_{CKM} is the Cabibbo-Kobayashi-Maskawa (CKM) quark-mixing matrix. The kinetic terms of the vLQ Lagrangians contain an extra parameter, κ [47],

$$\mathscr{L} \supset -\frac{1}{2} \chi^\dagger_{\mu v} \chi^{\mu v} + M^2_\chi \, \chi^\dagger_\mu \chi^\mu - i g_s \kappa \, \chi^\dagger_\mu T^a \chi_v \, G^{a\mu v}, \tag{15}$$

where $\chi_{\mu v}$ stands for the field-strength tensor of χ. The cross-section of the pair and single production of vLQs depends on κ.

IV. LHC PHENOMENOLOGY

We implement the phenomenological Lagrangian terms in FEYNRULES [48] to generate UNIVERSAL FEYNRULES OUTPUT (UFO) files [49] needed for MADGRAPH5 [50] to generate the signal and background events at the leading order. We use the default dynamical scale choice in MADGRAPH5 for event generation. Whenever available, we account for higher-order cross-sections with appropriate K factors. In particular, among the signal processes, we use a typical K-factor of 1.5 for the pair production of the sLQs [51–53]. We pass the parton-level events first through PYTHIA8 [54] for showering and hadronisation and then through DELPHES3 [55] for detector simulation with the default CMS card. The jets are reconstructed from the DELPHES tower objects with anti-k_T clustering algorithm [56] in FASTJET [57]. We use jets of two different radii in our analysis: (a) AK4 jets with $R = 0.4$ and (b) AK8 fatjets with $R = 0.8$.

A. Production at the LHC

As mentioned earlier, LQs can be produced at the LHC as resonances in pairs (mainly through strong interactions) or singly (mediated by the LQ-quark-RHN coupling, λ/Λ). Once produced, the LQs exclusively decay to RHN-jet pairs. A LQ can also appear in the t channel and contribute to the RHN pair production, $qq \to v_R v_R$. We show the cross-sections of different production processes for $M_{v_R} = 500$ GeV and $\lambda = 1$ (for sLQs) or $\Lambda = 1$ (for vLQs) with $\kappa = 0$ and 1 (the cross-sections of the LQ-production processes except the t-channel one increase with the extra $g\chi\chi$ coupling) in Fig. 1. The t-channel cross-sections are smaller than the pair and single LQ production cross-sections for lower LQ masses. Moreover, it is more suppressed for the sLQs than the vLQs. However, the $qq \to v_R v_R$ process becomes important for large couplings as its cross-section grows as λ^4 or Λ^4.[1] If LQs couple with the first-generation quarks, the RHN pair production cross-section gets an additional boost from the larger PDFs.

Since there is no direct experimental bound on the LQs decaying exclusively through RHNs, they can be even lighter than a TeV. In this paper, however, we mainly focus on the $M_{LQ} \geq 1$ TeV and $M_{v_R} \sim 500$ GeV region of the parameter space. In our computations, we include the contributions of all the above v_R-production processes to estimate the signal significance.

The RHN pair production processes can be classified in terms of the number of charged leptons in the final state:

(a) **Monolepton final state**: Ones with a muon accompanied by jet(s), fatjet(s) (from the hadronic decays of heavy bosons generated in the v_R decay), and some

---

[1] Though not significant for our study, the asymmetric pair production of the doublet LQs, where two different components are produced simultaneously, can also become non-negligible for very large couplings [58, 59].
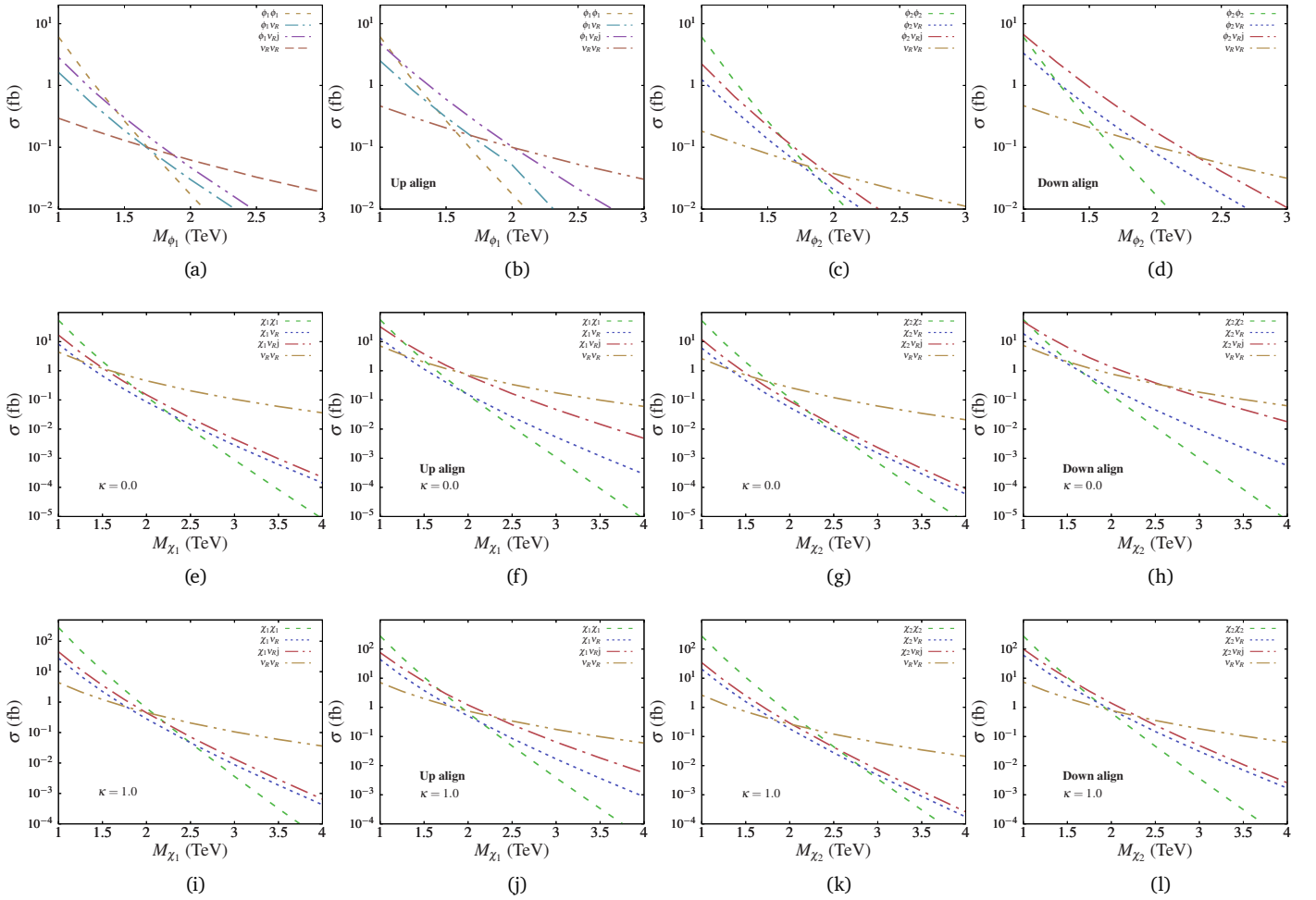
3

FIG. 1. Cross-sections of different production modes of sLQs [(a) – (d)] and vLQs with $\kappa = 0$ [(e) – (h)] and $\kappa = 1$ [(i) – (l)]. We also show the cross-section of RHN pair production through t-channel LQ exchange. The LQ single productions and RHN pair production process are computed for $\lambda(\Lambda) = 1$.

missing E_T. The different production modes contribute in the following manner:

$$pp \rightarrow \left\{ \begin{array}{l} \phi\phi/\chi\chi \\ \phi/\chi\,\nu_R\,(+j) \\ \nu_R\nu_R\,(+j) \end{array} \right\} \rightarrow \left\{ \begin{array}{l} (j\nu_R)(j\nu_R) \\ (j\nu_R)\nu_R\,(+j) \\ \nu_R\nu_R\,(+j) \end{array} \right\}$$
$$\rightarrow \mu^{\pm} W_h^{\mp} Z_h \nu_L + \text{jet(s)}.$$

(b) **Dilepton final state:** Ones with a opposite-sign muon pair ($\mu^+\mu^-$) plus jet(s) and fatjet(s). The different processes contribute to the dilepton final states as

$$pp \rightarrow \left\{ \begin{array}{l} \phi\phi/\chi\chi \\ \phi/\chi\,\nu_R\,(+j) \\ \nu_R\nu_R\,(+j) \end{array} \right\} \rightarrow \left\{ \begin{array}{l} (j\nu_R)(j\nu_R) \\ (j\nu_R)\nu_R\,(+j) \\ \nu_R\nu_R\,(+j) \end{array} \right\}$$
$$\rightarrow \left\{ \begin{array}{l} \mu^{\pm}\mu^{\mp} W_h^{\pm} W_h^{\mp} + \text{jet(s)} \\ \nu_L\nu_L Z_h Z_{\mu} + \text{jet(s)} \end{array} \right\}.$$

The subscripts h and μ denote the hadronic and leptonic decays of vector bosons, respectively. As shown above, a dimuon final state can arise in two ways. However, as one

applies the Z-veto cut to suppress the large Drell-Yan dilepton background, the signal events from the leptonic decays of Z are also cut out. In principle, one can also get more than two muons in the final state, where the extra leptons come from the decays of the vector bosons. However, since the leptonic branchings of the heavy vector bosons are smaller than their hadronic branchings, we do not consider final states with more than two muons.

In this paper, we follow a strategy of combining the contributions of multiple signal processes, which follows from our earlier papers [60, 61] where we showed how one could systematically combine pair and single production processes leading to the same final states without double counting. Later, in Refs. [33, 35, 46, 62], we further demonstrated the usefulness of it. Here, we extend this strategy to the pair production of RHNs.

B. Signals, cuts and the background

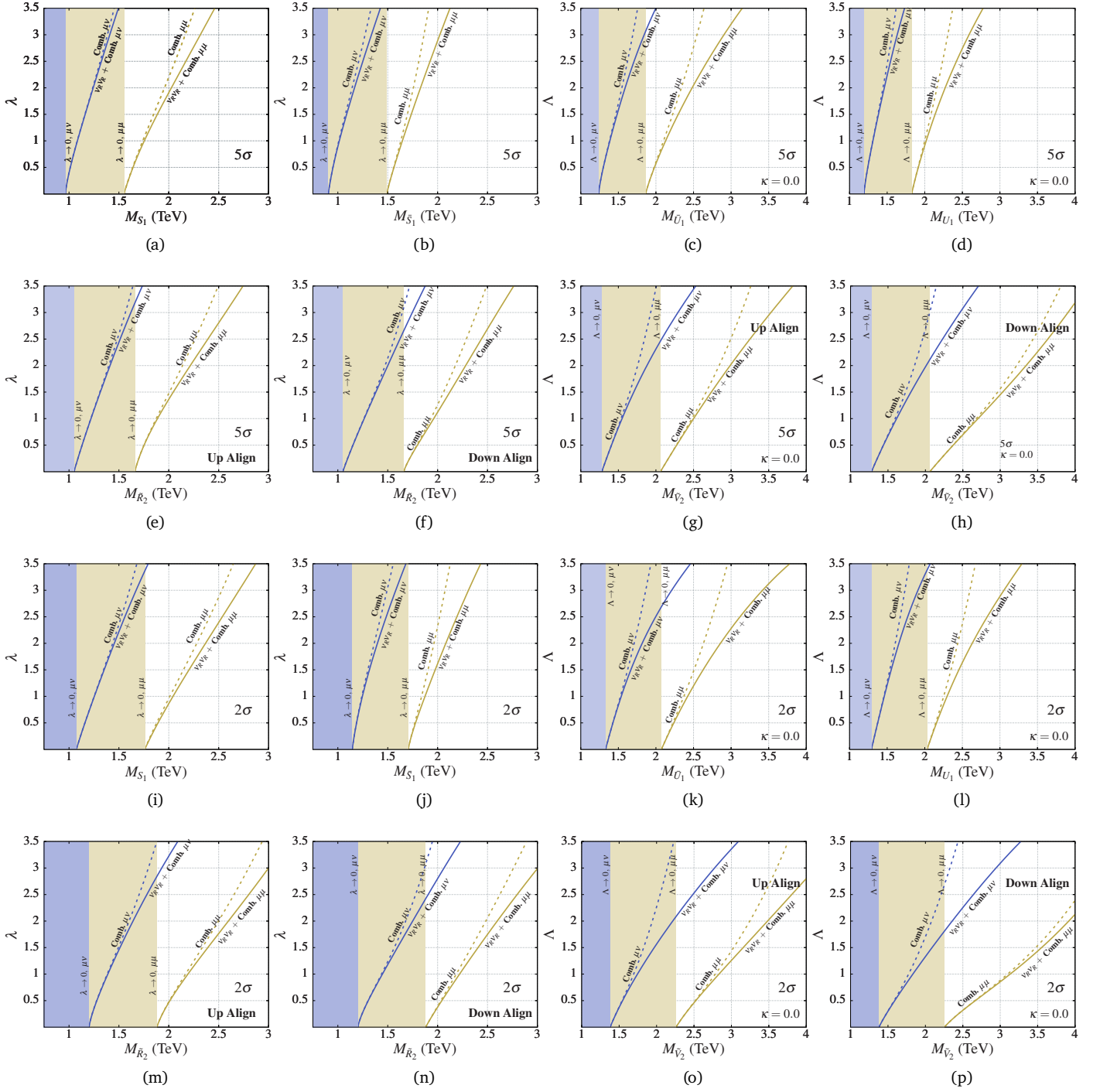We define our inclusive signal selection criteria for monolepton and dilepton events as:

FIG. 2. The least values of the new coupling (λ or Λ) needed to observe the signals with 5σ (top two rows) and 2σ (bottom two rows) significances as functions of masses at the HL-LHC. These plots are generated for $M_{\nu_R} = 500$ GeV and $\kappa = 0$ for the vLQS. The QCD regions (λ, $\Lambda \to 0$; dominated by LQ pair productions) in the monolepton and dilepton channels are shown with solid colours; the dashed lines are obtained by combining the LQ pair and single production events. Combining single-production events with pair-production events enhances the prospects. However, the prospects improve even further for high couplings since the RHN pair production via LQ exchange also contributes to the signals and enhances the significances (solid lines).

(a) A monolepton event must have

– exactly one high-p_T muon and

– at least one high-p_T AK4 jet and at least one AK8 fat-jet.

(b) A dilepton event must have

– a pair of opposite-sign muons, at least one of which should have high-p_T.

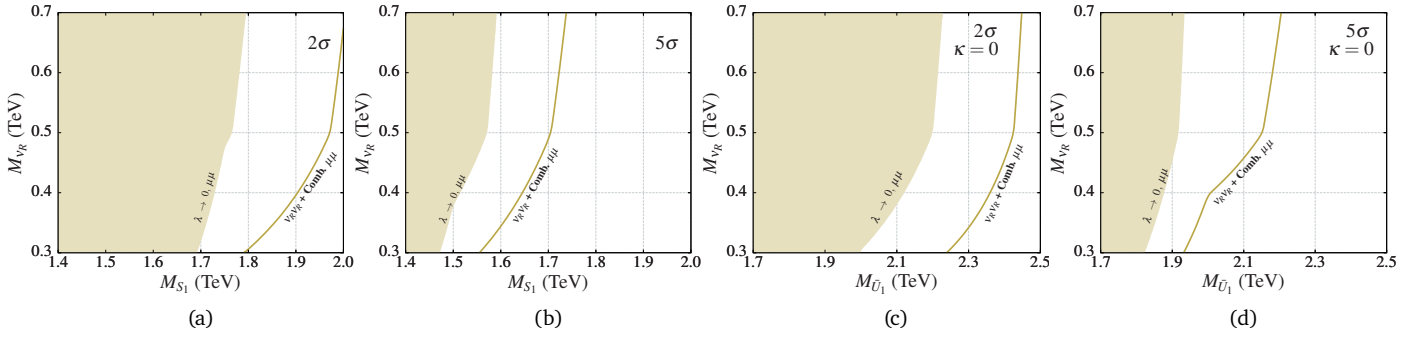– at least one high-p_T AK4 jet and at least one AK8 fat-jet.

5

FIG. 3. The [(a), (c)] 2σ and [(b), (d)] 5σ contours in the dilepton mode on the $M_{S_1}/M_{\bar{U}_1}$–M_{ν_R} plane. The combined contours are obtained for $\lambda, \Lambda = 1$.

TABLE I. Cross-sections of the major background processes without any cut. The higher-order cross-sections are taken from the literature; the corresponding QCD orders are shown in the last column. We use these cross-sections to compute the K factors to incorporate the higher-order effects.

Background processes		σ (pb)	QCD order
$V+$ jets [63, 64]	$Z+$ jets	6.33×10^4	N²LO
	$W+$ jets	1.95×10^5	NLO
$VV+$ jets [65]	$WW+$ jets	124.31	NLO
	$WZ+$ jets	51.82	NLO
	$ZZ+$ jets	17.72	NLO
Single t [66]	tW	83.10	N²LO
	tb	248.00	N²LO
	tj	12.35	N²LO
tt [67]	$tt+$ jets	988.57	N³LO
ttV [68]	ttZ	1.05	NLO+N²LL
	ttW	0.65	NLO+N²LL

The relevant background processes are listed in Table I. While generating the processes with very high cross-sections, we apply some basic generational-level cuts to save computation time. For the dilepton final state, the $W_\ell+$jets process can act as a background since a jet can be misidentified as a lepton. In fact, it is one of the major backgrounds for the RHN searches with same-sign dilepton final states. Since we consider only opposite-sign lepton pairs, in our case, its contribution is not important as the jet-faking-lepton efficiency is very small, $\sim 10^{-4}$ [69].

We show the cuts we apply on the two signals and the relevant backgrounds in Table II. In Table III, we show how these cuts affect various background processes. As examples, we also show the effect of the cuts on the signals for two ϕ_1 benchmarks.

V. HL-LHC PROSPECTS

We show the HL-LHC prospects of the mono- and dilepton channels for $M_{\nu_R} = 500$ GeV in Fig. 2 with the 5σ (discovery) and 2σ ($\sim$ exclusion) significance contours on the M_{LQ}–λ/Λ plane for each LQ mediator. We have used

the simple models introduced in Sec. III C to estimate the significances at 3 ab^{-1}; see Appendix A for our method of estimating the signal significance, $\mathscr{Z}$. (As explained, the mapping of the simple models to the actual models is straightforward for the singlet LQ models. For each doublet LQ, there are two possibilities depending on whether it is aligned with the up- or down-type quarks. However, from the cases covered in Fig. 1, we can map the simple models to the components of doublet LQs.) From the plots in Fig. 2, we see that, generally, the dilepton channel has better prospects than the monolepton one. This is because the branching ratio (BR) of the RHN in the $W\mu$ mode is roughly twice that of the $Z\nu$ mode, i.e., BR($\nu_R \to W^\pm\mu^\mp$)$\approx$ 2 BR($\nu_R \to Z\nu$), and the dilepton cuts lead to better yields due to the high μ-detection efficiency.

For the weak-singlet LQs and small values of λ or Λ (small to suppress the LQ single productions and the t-channel LQ exchange but not enough to form displaced vertices), the 5σ discovery reaches for S_1 and $\bar{S}_1$ in the pair production mode in the dilepton channel can go as high as 1.6 and 1.5 TeV, respectively. But, for $\lambda = 1$, the reaches enhance to 1.8 and 1.6 TeV once the single production and the t-channel RHN-pair production contributions are combined in the signal. For $\bar{U}_1$ and U_1, the 5σ reaches in the pair-only mode are about 1.9 and 1.8 TeV, respectively, for the same RHN mass and $\kappa = 0$, which increase to 2.1 and 2.0 TeV when the single production events are combined in the signal. For $\lambda = 1$, the actual reaches are slightly better as the $qq \to \nu_R\nu_R$ process also contributes. As expected, the t-channel process becomes important only for large couplings.

In the absence of discovery, the 2σ values provide rough estimates of the exclusion limits. For $M_{\nu_R} = 500$ GeV, the HL-LHC can exclude up to 2.0 and 1.9 TeV in the cases of S_1 and $\bar{S}_1$, respectively. The exclusion limits for $\bar{U}_1$ and U_1 for $\kappa = 0$ are 2.4 and 2.3 TeV, respectively.

The vLQ numbers shown in Fig. 2 should be considered conservative as we have put the extra gauge coupling to zero. Their prospects improve if this coupling is nonzero. For example, if $\kappa = 1$, the 5σ reaches for $\bar{U}_1$ and U_1 go to about 2.2 and 2.1 TeV, respectively, in the pair-only mode and to about 2.4 and 2.2 TeV in the combined mode (for $\Lambda = 1$). Similarly, the 2σ limits change to 2.6 and 2.5 TeV, respectively (for $\Lambda = 1$). The enhancement in each mode

TABLE II. The selection cuts applied on the monolepton and dilepton final states. The b veto reduces the top backgrounds and fj denotes a fatjet.

Selection cuts	Channel	
	Monolepton	Dilepton
$\mathfrak{C}_1$: Selection of high p_T Leptons and jets	$p_T(\mu) > 200$ GeV, $p_T(j_1) > 200$ GeV, No b-tagged jet	$p_T(\mu) > 220$ GeV, $p_T(j_1) > 200$ GeV, No b-tagged jet
$\mathfrak{C}_2$: Identification of fatjet	$p_T(\text{fj}) > 80$ GeV, $\tau_{21} < 0.3$, $65 < M(\text{fj}) < 100$ GeV, $\Delta R(\text{fj}, \mu) > 1.0$	$p_T(\text{fj}_{\phi(\chi)}) > 120\,(180)$ GeV, $\tau_{21} < 0.3$, $65 < M(\text{fj}) < 100$ GeV, $\Delta R(\text{fj}, \mu) > 0.8$
$\mathfrak{C}_3$: Dilepton invariant mass	—	$M(\mu, \mu) > 150$ GeV
$\mathfrak{C}_4$: Scalar cuts	$S_T > 1200$ GeV, $\not{E}_T > 150$ GeV, $\text{fj}_{\text{H}_\text{T}} > 600$ GeV	$S_T > 1400$ GeV, $\text{fj}_{\text{H}_\text{T}} > 600$ GeV

TABLE III. Cut flows for two ϕ_1 benchmarks ($\lambda \to \{0, 1\}$) and the relevant background processes at luminosity $\mathscr{L} = 3$ ab^{-1}.

■ **Monolepton final state**	Selection cuts			
	$\mathfrak{C}_1$	$\mathfrak{C}_2$	$\mathfrak{C}_3$	$\mathfrak{C}_4$
Signal benchmarks				
$M_{\phi_1} = 1250$ GeV, $M_{\nu_R} = 500$ GeV (pair production)	270	126	126	106
$M_{\phi_1} = 1250$ GeV, $M_{\nu_R} = 500$ GeV (single production)	291	159	159	117
			Total number of monolepton signal events:	223
Background processes				
$W_\ell\,(+2j)$	4.53×10^7	2.02×10^6	2.02×10^6	39346
$W_\ell Z_h\,(+2j)$	2.55×10^5	74148	74148	3895
$Z_\ell\,(+2j)$	1.46×10^7	7.93×10^5	7.93×10^5	2640
$W_\ell W_h\,(+2j)$	2.00×10^5	71229	71229	2483
$t_h W_\ell + t_\ell W_h$	1.52×10^5	45436	45436	1729
$t_\ell + b/j$	3313	555	555	22
			Total number of background events:	50115
■ **Dilepton final state**	Selection cuts			
	$\mathfrak{C}_1$	$\mathfrak{C}_2$	$\mathfrak{C}_3$	$\mathfrak{C}_4$
Signal benchmarks				
$M_{\phi_1} = 1250$ GeV, $M_{\nu_R} = 500$ GeV (pair production)	339	166	119	118
$M_{\phi_1} = 1250$ GeV, $M_{\nu_R} = 500$ GeV (single production)	194	113	73	70
			Total number of dilepton signal events:	188
Background processes				
$W_\ell Z_\ell\,(+2j)$	39685	2125	632	101
$W_\ell W_\ell\,(+2j)$	31093	1422	514	51
$t_\ell W_\ell$	19694	1062	218	28
$t_\ell t_\ell\,(+2j)$	21256	1097	60	20
			Total number of background events:	200

is proportional to the corresponding improvement in the cross-section (see Fig. 1).

The results are more promising for the doublet LQ models for two reasons. First, our selection criteria are insensitive towards the charge of the LQ. As a result, the contributions of the individual components to the signal add up. Second, one component of the doublets (either charge 1/3 or 2/3, depending on how the LQ is aligned) couples with a first-generation quark through the CKM mixing, which boosts the cross-sections. For $\lambda = 1$, the discovery reaches for both up-aligned $\tilde{R}_2$ (one with flavour off-diagonal couplings to the down-type quarks) and down-aligned $\tilde{R}_2$ (one with flavour off-diagonal couplings to the up-type quarks)

go up to about 1.9 TeV in the dilepton channel. Similarly, for $\Lambda = 1$ and $\kappa = 0$, the discovery reaches for up-aligned and down-aligned $\tilde{V}_2$ go up to 2.5 and 3.0 TeV, respectively. As expected, in the high coupling regions, the signal enhancements from the $qq \to \nu_R \nu_R$ process are more pronounced in the doublet cases than the singlet ones due to the first-generation quark in the initial states. Similar trends are observed in the doublet-LQ exclusion plots as well.

We draw the 2σ and 5σ contours on the $M_{S_1, \bar{U}_1}$–M_{ν_R} planes in Fig. 3 to demonstrate how the signal significance varies with M_{ν_R}. Since the RHNs appear only in the decay, we do not expect any significant dependence on M_{ν_R}
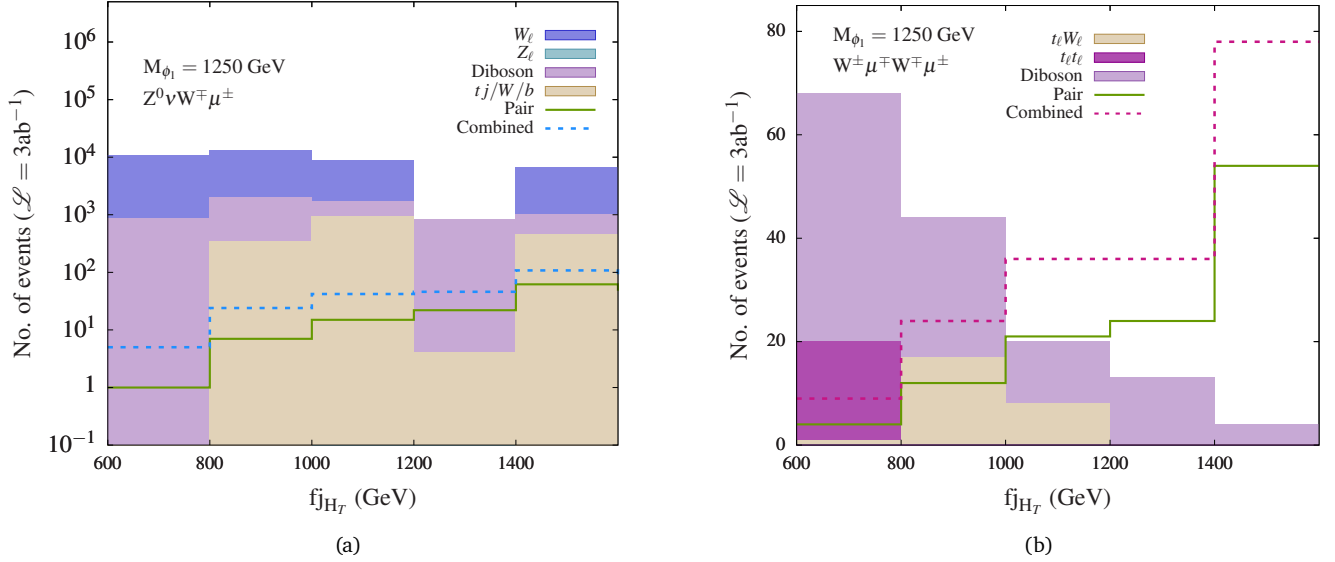
FIG. 4. The distribution of signal and background events in (a) the monolepton channel and (b) the dilepton channel. The events are first passed through $\mathfrak{C}_1$–$\mathfrak{C}_4$ (Table II) and then binned according to fj_{H_T} (the scalar sum of the transverse momenta of the fatjets). The fifth bin is open on the higher side, i.e., $\mathrm{fj}_{H_T}^{(5)} > 1400$ GeV. The total number of events for every process is reported in the last row of Table III.

VI. SUMMARY AND CONCLUSIONS

In this paper, we analysed the LQ-mediated pair production of RHNs at the LHC. This channel has received little attention in the literature and is yet to be explored experimentally. This is an interesting signal to probe if RHNs are within the TeV scale, a possibility realisable with the inverse seesaw mechanism for a wide range of neutrino parameters. In this mechanism, the RHNs are pseudo-Dirac type and are not restricted by the stringent same-sign dilepton-search bounds. Moreover, no direct experimental limits exist on LQs that exclusively couple with RHNs.

LQs can contribute to the RHN pair productions in two ways: 1) the RHNs come from the decay of LQs if they are lighter than the LQs, and 2) a t-channel LQ exchange can produce a pair of RHNs in the quark-fusion process. Since the LQs can be resonantly produced either in pairs or singly, we have three processes to produce RHN pairs. These three processes become significant in different regions of the parameter space. The mostly QCD-mediated LQ pair productions are dominant if the LQs are not very heavy and the new couplings λ, Λ are not very large. The t-channel processes are significant if λ, Λ are large ($\gtrsim 2$) and the exchanged LQs are very heavy (the resonant productions are beyond the reach of LHC). LQ single productions are important in the intermediate mass range (single pro-

ductions of heavy particles are less phase-space-suppressed than the pair production) if $\lambda, \Lambda \gtrsim \mathscr{O}(1)$.

Extending a strategy we proposed earlier, we defined the signals so that all three processes contribute to the signals, thus proving a complete coverage of the parameter space within the reach of the HL-LHC. However, for a conservative estimation of the HL-LHC prospects, we focused only on second-generation interactions in this paper. Our signals have either an opposite-sign muon pair or a single muon along with hadronically decaying bosons. We analysed the prospects of these channels at the HL-LHC and obtained the 5σ and 2σ significance contours.

We found that LQ-mediated RHN production has excellent prospects at the HL-LHC. For scalar LQs, the discovery reaches vary from about 1 TeV to close to 3 TeV. For vector LQs, they are between 2 TeV to 4 TeV. Our analysis is generic and comprehensive as 1) we do not assume any specific property of the RHN except that it is lighter than a TeV and is pseudo-Dirac type (because of ISM) decaying to either a W boson and a muon or a Z/H boson and a neutrino, and 2) we considered all possible scalar and vector LQs that can exclusively couple to the second-generation RHN.

MODEL FILES

The UFO model files are available at https://github.com/rsrchtsm/LQ_RHN.

Appendix A: Estimating $\mathscr{Z}$ score

We showed how one could make use of the distribution of the data (rather than just the total number of events) to

estimate the signal significance in Ref. [46]. We follow the method outlined there. After passing the events through the cuts in Table II, we first bin the data by the scalar sum of the transverse momenta of the fatjets, fj_{H_T} (see Fig. 4). We then estimate the combined signal significance by Liptak-Stouffer (weighted) $\mathscr{Z}$ score [71, 72]:

$$\mathscr{Z} = \frac{\sum_{i=1}^5 w_i \mathscr{Z}_i}{\sqrt{\sum_{i=1}^5 w_i^2}}. \qquad \text{(A1)}$$

Here, $\mathscr{Z}_i$ is the signal significance score in the ith bin ($i \in \{1,2,3,4,5\}$) computed as [73]

$$\mathscr{Z}_i = \sqrt{2\left(N_S^i + N_B^i\right)\ln\left(\frac{N_S^i + N_B^i}{N_B^i}\right) - 2N_S^i}, \qquad \text{(A2)}$$

where N_S^i and N_B^i are the numbers of signal and background events in the bin. The corresponding weight is denoted as w_i. The weight is commonly taken as the inverse of the variance [74]. We set w_i equal to the inverse of the square of the total error in the background events in the ith bin, i.e., $w_i^{-1} = (\text{statistical error})^2 = N_B^i$.

[1] P. Minkowski, *μ → eγ at a Rate of One Out of 10^9 Muon Decays?*, *Phys. Lett. B* **67** (1977) 421–428.

[2] R. N. Mohapatra and G. Senjanovic, *Neutrino Mass and Spontaneous Parity Nonconservation*, *Phys. Rev. Lett.* **44** (1980) 912.

[3] R. N. Mohapatra, *Mechanism for Understanding Small Neutrino Mass in Superstring Theories*, *Phys. Rev. Lett.* **56** (1986) 561–563.

[4] R. N. Mohapatra and J. W. F. Valle, *Neutrino Mass and Baryon Number Nonconservation in Superstring Models*, *Phys. Rev. D* **34** (1986) 1642.

[5] S. Banerjee, P. S. B. Dev, A. Ibarra, T. Mandal and M. Mitra, *Prospects of Heavy Neutrino Searches at Future Lepton Colliders*, *Phys. Rev. D* **92** (2015) 075002, [1503.05491].

[6] W.-Y. Keung and G. Senjanovic, *Majorana Neutrinos and the Production of the Right-handed Charged Gauge Boson*, *Phys. Rev. Lett.* **50** (1983) 1427.

[7] M. Thomas Arun, T. Mandal, S. Mitra, A. Mukherjee, L. Priya and A. Sampath, *Testing left-right symmetry with an inverse seesaw mechanism at the LHC*, *Phys. Rev. D* **105** (2022) 115007, [2109.09585].

[8] A. Ekstedt, R. Enberg, G. Ingelman, J. Löfgren and T. Mandal, *Constraining minimal anomaly free U(1) extensions of the Standard Model*, *JHEP* **11** (2016) 071, [1605.04855].

[9] D. Choudhury, K. Deka, T. Mandal and S. Sadhukhan, *Neutrino and Z′ phenomenology in an anomaly-free U(1) extension: role of higher-dimensional operators*, *JHEP* **06** (2020) 111, [2002.02349].

[10] K. Deka, T. Mandal, A. Mukherjee and S. Sadhukhan, *Leptogenesis in an anomaly-free U(1) extension with higher-dimensional operators*, 2105.15088.

[11] M. T. Arun, A. Chatterjee, T. Mandal, S. Mitra, A. Mukherjee and K. Nivedita, *Search for the Z' boson decaying to a right-handed neutrino pair in leptophobic U(1) models*, *Phys. Rev. D* **106** (2022) 095035, [2204.02949].

[12] J. C. Pati and A. Salam, *Lepton Number as the Fourth Color*, *Phys. Rev.* **D10** (1974) 275–289. [Erratum: Phys. Rev.D11,703(1975)].

[13] H. Georgi and S. L. Glashow, *Unity of All Elementary Particle Forces*, *Phys. Rev. Lett.* **32** (1974) 438–441.

[14] B. Schrempp and F. Schrempp, *Light Leptoquarks*, *Phys. Lett.* **B153** (1985) 101–107.

[15] R. Barbier et al., *R-parity violating supersymmetry*, *Phys. Rept.* **420** (2005) 1–202, [hep-ph/0406039].

[16] L. Calibbi, A. Crivellin and T. Li, *Model of vector leptoquarks in view of the B-physics anomalies*, *Phys. Rev. D* **98** (2018) 115002, [1709.00692].

[17] M. Blanke and A. Crivellin, *B Meson Anomalies in a Pati-Salam Model within the Randall-Sundrum Background*, *Phys. Rev. Lett.* **121** (2018) 011801, [1801.07256].

[18] A. Azatov, D. Barducci, D. Ghosh, D. Marzocca and L. Ubaldi, *Combined explanations of B-physics anomalies: the sterile neutrino solution*, *JHEP* **10** (2018) 092, [1807.10745].

[19] T. Mandal, S. Mitra and S. Raz, *$R_{D^{(*)}}$ motivated $\mathscr{S}_1$ leptoquark scenarios: Impact of interference on the exclusion limits from LHC data*, *Phys. Rev. D* **99** (2019) 055028, [1811.03561].

[20] U. Aydemir, T. Mandal and S. Mitra, *Addressing the $\mathbf{R}_{D^{(*)}}$ anomalies with an $\mathbf{S}_1$ leptoquark from SO(10) grand unification*, *Phys. Rev. D* **101** (2020) 015011, [1902.08108].

[21] S. Balaji and M. A. Schmidt, *Unified SU(4) theory for the $R_{D^{(*)}}$ and $R_{K^{(*)}}$ anomalies*, *Phys. Rev. D* **101** (2020) 015026, [1911.08873].

[22] A. Crivellin, D. Müller and F. Saturnino, *Flavor Phenomenology of the Leptoquark Singlet-Triplet Model*, *JHEP* **06** (2020) 020, [1912.04224].

[23] A. Crivellin, D. Müller and F. Saturnino, *Leptoquarks in oblique corrections and Higgs signal strength: status and prospects*, *JHEP* **11** (2020) 094, [2006.10758].

[24] A. Crivellin, D. Mueller and F. Saturnino, *Correlating $h\mu^+\mu^-$ to the Anomalous Magnetic Moment of the Muon via Leptoquarks*, *Phys. Rev. Lett.* **127** (2021) 021801, [2008.02643].

[25] A. Bhaskar, D. Das, T. Mandal, S. Mitra and C. Neeraj, *Precise limits on the charge-2/3 U1 vector leptoquark*, *Phys. Rev. D* **104** (2021) 035016, [2101.12069].

[26] A. Bhaskar, A. A. Madathil, T. Mandal and S. Mitra, *Combined explanation of W-mass, muon g-2, RK(*) and RD(*) anomalies in a singlet-triplet scalar leptoquark model*, *Phys. Rev. D* **106** (2022) 115009, [2204.09031].

[27] A. Das and N. Okada, *Inverse seesaw neutrino signatures at the LHC and ILC*, *Phys. Rev. D* **88** (2013) 113001, [1207.3734].

[28] B. Dumont, K. Nishiwaki and R. Watanabe, *LHC constraints and prospects for S_1 scalar leptoquark explaining the $\bar{B} \to D^{(*)}\tau\bar{\nu}$ anomaly*, *Phys. Rev. D* **94** (2016) 034001, [1603.05248].

[29] A. Das and N. Okada, *Bounds on heavy Majorana neutrinos in type-I seesaw and implications for collider searches*, *Phys. Lett. B* **774** (2017) 32–40, [1702.04668].

[30] U. K. Dey, D. Kar, M. Mitra, M. Spannowsky and A. C. Vincent, *Searching for Leptoquarks at IceCube and the LHC*, *Phys. Rev. D* **98** (2018) 035014, [1709.02009].

[31] P. Bandyopadhyay and R. Mandal, *Revisiting scalar leptoquark at the LHC*, *Eur. Phys. J. C* **78** (2018) 491, [1801.04253].

[32] A. Das, S. Jana, S. Mandal and S. Nandi, *Probing right handed neutrinos at the LHeC and lepton colliders using fat jet signatures*, *Phys. Rev. D* **99** (2019) 055030, [1811.04291].

[33] K. Chandak, T. Mandal and S. Mitra, *Hunting for scalar leptoquarks with boosted tops and light leptons*, *Phys. Rev. D* **100** (2019) 075019, [1907.11194].

[34] R. Padhan, S. Mandal, M. Mitra and N. Sinha, *Signatures of $\tilde{R}_2$ class of Leptoquarks at the upcoming ep colliders*, *Phys. Rev. D* **101** (2020) 075037, [1912.07236].

[35] A. Bhaskar, T. Mandal and S. Mitra, *Boosting vector leptoquark searches with boosted tops*, *Phys. Rev. D* **101** (2020) 115015, [2004.01096].

[36] S. Iguro, M. Takeuchi and R. Watanabe, *Testing leptoquark/EFT in $\bar{B} \to D^{(*)}l\bar{\nu}$ at the LHC*, *Eur. Phys. J. C* **81** (2021) 406, [2011.02486].

[37] N. Ghosh, S. K. Rai and T. Samui, *Collider Signatures of a Scalar Leptoquark and Vector-like Lepton in Light of Muon Anomaly*, 2206.11718.

[38] N. Desai and A. Sengupta, *Status of leptoquark models after LHC Run-2 and discovery prospects at future colliders*, 2301.01754.

[39] **ATLAS** collaboration, G. Aad et al., *Search for pairs of scalar leptoquarks decaying into quarks and electrons or muons in $\sqrt{s}$ = 13 TeV pp collisions with the ATLAS detector*, *JHEP* **10** (2020) 112, [2006.05872].

[40] **ATLAS** collaboration, *Search for pair-produced scalar and vector leptoquarks decaying into third-generation quarks and first- or second-generation leptons in pp collisions with the ATLAS detector*, 2210.04517.

[41] D. Das, K. Ghosh, M. Mitra and S. Mondal, *Probing sterile neutrinos in the framework of inverse seesaw mechanism through leptoquark productions*, *Phys. Rev. D* **97** (2018) 015024, [1708.06206].

[42] S. Mandal, M. Mitra and N. Sinha, *Probing leptoquarks and heavy neutrinos at the LHeC*, *Phys. Rev. D* **98** (2018) 095004, [1807.06455].

[43] A. Bhaskar, D. Das, B. De and S. Mitra, *Enhancing scalar productions with leptoquarks at the LHC*, *Phys. Rev. D* **102** (2020) 035002, [2002.12571].

[44] G. Cottin, O. Fischer, S. Mandal, M. Mitra and R. Padhan, *Displaced neutrino jets at the LHeC*, *JHEP* **06** (2022) 168, [2104.13578].

[45] A. Bhaskar, D. Das, B. De, S. Mitra, A. K. Nayak and C. Neeraj, *Leptoquark-assisted singlet-mediated di-Higgs production at the LHC*, *Phys. Lett. B* **833** (2022) 137341, [2205.12210].

[46] A. Bhaskar, T. Mandal, S. Mitra and M. Sharma, *Improving third-generation leptoquark searches with combined signals and boosted top quarks*, *Phys. Rev. D* **104** (2021) 075037, [2106.07605].

[47] I. Doršner, S. Fajfer, A. Greljo, J. F. Kamenik and N. Košnik, *Physics of leptoquarks in precision experiments and at particle colliders*, *Phys. Rept.* **641** (2016) 1–68, [1603.04993].

[48] A. Alloul, N. D. Christensen, C. Degrande, C. Duhr and B. Fuks, *FeynRules 2.0 - A complete toolbox for tree-level phenomenology*, *Comput. Phys. Commun.* **185** (2014) 2250–2300, [1310.1921].

[49] C. Degrande, C. Duhr, B. Fuks, D. Grellscheid, O. Mattelaer and T. Reiter, *UFO - The Universal FeynRules Output*, *Comput. Phys. Commun.* **183** (2012) 1201–1214, [1108.2040].

[50] J. Alwall, R. Frederix, S. Frixione, V. Hirschi, F. Maltoni, O. Mattelaer et al., *The automated computation of tree-level and next-to-leading order differential cross sections, and their matching to parton shower simulations*, *JHEP* **07** (2014) 079, [1405.0301].

[51] M. Kramer, T. Plehn, M. Spira and P. M. Zerwas, *Pair production of scalar leptoquarks at the CERN LHC*, *Phys. Rev. D* **71** (2005) 057503, [hep-ph/0411038].

[52] T. Mandal, S. Mitra and S. Seth, *Pair Production of Scalar Leptoquarks at the LHC to NLO Parton Shower Accuracy*, *Phys. Rev. D* **93** (2016) 035018, [1506.07369].

[53] C. Borschensky, B. Fuks, A. Jueid and A. Kulesza, *Scalar leptoquarks at the LHC and flavour anomalies: a comparison of pair-production modes at NLO-QCD*, *JHEP* **11** (2022) 006, [2207.02879].

[54] T. Sjöstrand, S. Ask, J. R. Christiansen, R. Corke, N. Desai, P. Ilten et al., *An introduction to PYTHIA 8.2*, *Comput. Phys. Commun.* **191** (2015) 159–177, [1410.3012].

[55] **DELPHES 3** collaboration, J. de Favereau, C. Delaere, P. Demin, A. Giammanco, V. Lemaître, A. Mertens et al., *DELPHES 3, A modular framework for fast simulation of a generic collider experiment*, *JHEP* **02** (2014) 057, [1307.6346].

[56] M. Cacciari, G. P. Salam and G. Soyez, *The anti-k_t jet clustering algorithm*, *JHEP* **04** (2008) 063, [0802.1189].

[57] M. Cacciari, G. P. Salam and G. Soyez, *FastJet User Manual*, *Eur. Phys. J. C* **72** (2012) 1896, [1111.6097].

[58] I. Doršner, A. Lejlić and S. Saad, *Asymmetric leptoquark pair production at LHC*, *JHEP* **03** (2023) 025, [2210.11004].

[59] I. Doršner, S. Fajfer and A. Lejlić, *Novel Leptoquark Pair Production at LHC*, *JHEP* **05** (2021) 167, [2103.11702].

[60] T. Mandal and S. Mitra, *Probing Color Octet Electrons at the LHC*, *Phys. Rev. D* **87** (2013) 095008, [1211.6394].

[61] T. Mandal, S. Mitra and S. Seth, *Single Productions of Colored Particles at the LHC: An Example with Scalar Leptoquarks*, *JHEP* **07** (2015) 028, [1503.04689].

[62] T. Mandal, S. Mitra and S. Seth, *Probing Compositeness with the CMS $eejj$ & eej Data*, *Phys. Lett. B* **758** (2016) 219–225, [1602.01273].

[63] S. Catani, L. Cieri, G. Ferrera, D. de Florian and M. Grazzini, *Vector boson production at hadron colliders: a fully exclusive QCD calculation at NNLO*, *Phys. Rev. Lett.* **103** (2009) 082001, [0903.2120].

[64] G. Balossini, G. Montagna, C. M. Carloni Calame, M. Moretti, O. Nicrosini, F. Piccinini et al., *Combination of electroweak and QCD corrections to single W production at the Fermilab Tevatron and the CERN LHC*, *JHEP* **01** (2010) 013, [0907.0276].

[65] J. M. Campbell, R. K. Ellis and C. Williams, *Vector boson pair production at the LHC*, *JHEP* **07** (2011) 018, [1105.0020].

[66] N. Kidonakis, *Theoretical results for electroweak-boson and single-top production*, *PoS* **DIS2015** (2015) 170, [1506.04072].

[67] C. Muselli, M. Bonvini, S. Forte, S. Marzani and G. Ridolfi, *Top Quark Pair Production beyond NNLO*, *JHEP* **08** (2015)

076, [1505.02006].

[68] A. Kulesza, L. Motyka, D. Schwartländer, T. Stebel and V. Theeuwes, *Associated production of a top quark pair with a heavy electroweak gauge boson at NLO+NNLL accuracy*, *Eur. Phys. J. C* **79** (2019) 249, [1812.08622].

[69] D. Curtin, J. Galloway and J. G. Wacker, *Measuring the $t\bar{t}h$ coupling from same-sign dilepton $+2b$ measurements*, *Phys. Rev. D* **88** (2013) 093006, [1306.5695].

[70] M. Mitra, R. Ruiz, D. J. Scott and M. Spannowsky, *Neutrino Jets from High-Mass W_R Gauge Bosons in TeV-Scale Left-Right Symmetric Models*, *Phys. Rev. D* **94** (2016) 095016, [1607.03504].

[71] S. A. Stouffer, E. A. Suchman, L. C. DeVinney, S. A. Star and R. M. Williams Jr., *The American Soldier, Vol.1: Adjustment during Army Life*. Princeton University Press, Princeton, 1949.

[72] T. Lipták, *On the combination of independent tests*, *Magyar Tud Akad Mat Kutato Int Kozl* **3** (1958) 171–197.

[73] G. Cowan, K. Cranmer, E. Gross and O. Vitells, *Asymptotic formulae for likelihood-based tests of new physics*, *Eur. Phys. J. C* **71** (2011) 1554, [1007.1727]. [Erratum: Eur.Phys.J.C 73, 2501 (2013)].

[74] M. C. Whitlock, *Combining probability from independent tests: the weighted z-method is superior to fisher's approach*, *Journal of Evolutionary Biology* **18** (2005) 1368–1373.